Alloying and Microstructural Management in Developing SMAW Electrodes for HSLA-100 Steel

To determine the optimal composition of SMAW electrodes for use with HSLA-100 steel, three sets of experimental welding electrodes were developed

BY W. WANG and S. LIU

Abstract. Due to the excellent mechanical properties of high-strength, low-alloy (HSLA) plate steels, fabricators and manufacturers have great interest in the development of high-performance welding electrodes for these steels.

Three sets of experimental welding electrodes were designed and manufactured for this research. The first iteration of electrodes was targeted to vary copper from 0.0 to 3.7 wt-%. In the second iteration, chromium was removed and the Ni and Cu contents were adjusted to the ranges of 1.0–3.0 and 1.0–1.5 wt-%, respectively. Niobium was added at 0.03 wt-%. The third iteration lowered the carbon content to 0.03 wt-% and reduced the nitrogen content to 100 ppm maximum. Nickel and copper contents were fine-tuned to 1.0 to 2.3 and 0.8 to 1.0 wt-%, respectively. Standard light and electron metallographic techniques were used to examine the weld metal microstructural evolution. Electron diffraction patterns from the different phases were analyzed. Mechanical testing was performed to characterize the resulting welds.

The optimal composition for the HSLA-100 steel weld metals was determined as 0.04 wt-% C, 1.3 wt-% Mn, 2.3 wt-% Ni, 0.55 wt-% Mo, 0.8 wt-% Cu, 90 ppm N, and 270 ppm O. The 0.03 wt-% Nb worked well with Cu to develop synergistic precipitation, which uniformized the hardness fluctuations on weld cross sections. The weld metals that exhibited a predominantly acicular ferrite (AF) structure with some coarse granular bainite presented the best toughness properties. Weld metals with the above composition easily met the U.S. Navy requirement for HSLA-100 steel welds in this work.

W. WANG is with Consumables R&D, The Lincoln Electric Co., Cleveland, Ohio. S. LIU is with the Center for Welding, Joining & Coatings Research, Colorado School of Mines, Golden, Colo.

Introduction

To meet more stringent fabrication requirements, welding consumable development for modern HSLA steels faces a strong challenge. As an example, the U.S. Navy has shown interest in developing shielded metal arc welding (SMAW) electrodes that could produce both high yield strength (about 100 ksi and 690 MPa) and excellent Charpy V-notch impact toughness, no less than 35 ft-lb (47 J at –60°F), for HSLA-100 steel weld metal.

It is well established that Charpy V-notch impact toughness generally decreases with increasing tensile strength of a structural steel weld metal. Grain refinement, nevertheless, can increase both strength and toughness of a weld metal. Since alloying elements in a weld metal play important roles in microstructural evolution, including grain refinement, an appropriate alloying strategy becomes critical to promote a desirable microstructural distribution and to achieve specification requirements. Hence, the effect of major alloying elements, *e.g.*, C, Mn, Si, N, O, S, H, etc., needs to be examined for the development of a successful alloy system for HSLA-100 steel weld metal.

KEY WORDS

Shielded Metal Arc Welding
SMAW
High-Strength, Low-Alloy Steel
HSLA-100
Acicular Ferrite
Granular Bainite
Impact Toughness

Carbon, with its strong hardening effect, increases the volume percentage of hard microstructures, *e.g.*, martensite, in a steel weld. Nitrogen and oxygen are important elements that precipitate and form inclusions that may or may not be beneficial to the final microstructures and mechanical properties of a weld. Sulfur and hydrogen are the key elements in determining hot and cold cracking behavior and, finally, manganese and silicon are the deoxidizers and solid-solution strengtheners. Evans (Refs. 1, 2) has reported that changing the content of manganese or silicon can dramatically affect the microstructural distribution in a weld metal. Additionally, due to their direct effect on slag performance and welding operability, the amounts of Mn and Si in the flux formulation, later transferred to the weld metal, must be strictly controlled. It is commonly accepted that ranges of manganese and silicon in low carbon steel weld metals are about 1.4 and 0.2 to 0.45 wt-%, respectively.

Effect of Aluminum and Its Interaction with O and Ti

Aluminum is an effective deoxidizer and denitrider (Ref. 3). Grong and Matlock (Ref. 4) reported in 1985 that for submerged arc (SA) welding of plain carbon steel at a heat input of 4.9 kJ/mm, an optimal Charpy V-notch impact toughness was achieved when [Al wt-%]/[O wt-%]^2 is equal to 28. Brownlee (Ref. 5) further determined the [Al wt-%]/[O wt-%] ratio significantly affected the volume fractions of inclusions. For large inclusions with diameters greater than 0.5 mm, their volume fractions increased with the ratio; however, for small inclusions with diameters less than 0.5 mm, the

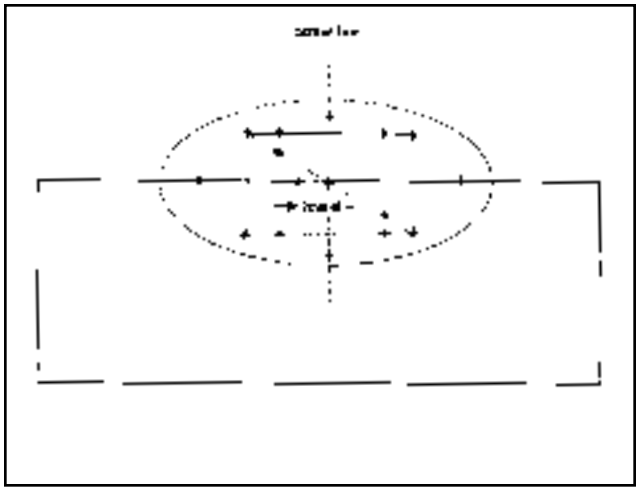

Fig. 1 — The hardness survey on the cross section of weldments.

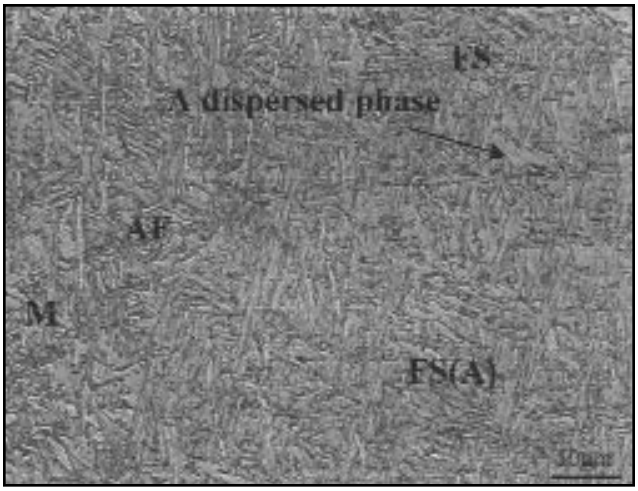

Fig. 2 — A typical HSLA-100 weldment microstructure under light microscope.

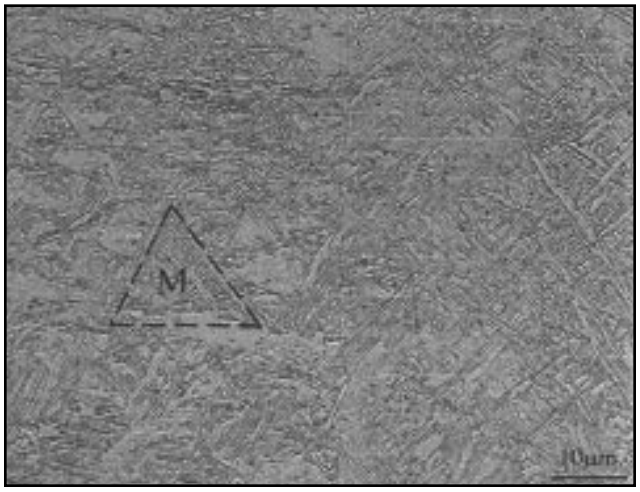

Fig. 3 — The morphology of lath martensite under light microscope.

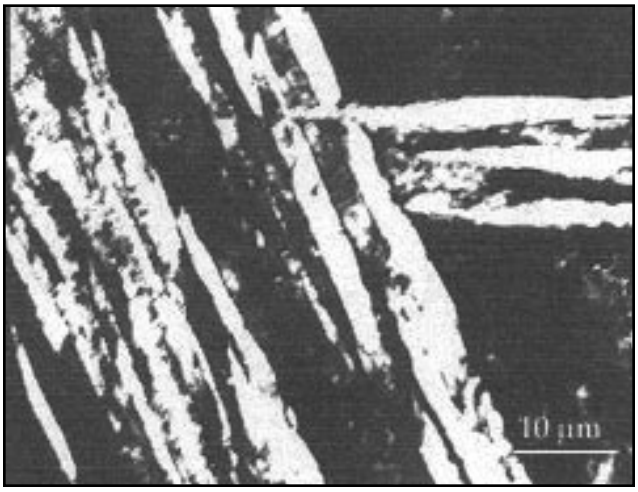

Fig. 4 — TEM morphology of FS(A) phase.

opposite trend was observed. Regarding microstructure, large inclusions promoted formation of acicular ferrite (AF); and small precipitates, such as AlN, pinned the austenite grain boundaries for grain refinement. The optimum conditions for acicular ferrite nucleation could be achieved when the [Al wt-%]/[O wt-%] ratio was between 0 and 1.1. On the other hand, when Ti was introduced into the weld metal, it promoted formation of acicular ferrite by minimizing grain boundary ferrite if the aluminum content was lower than 0.04 wt-%; however, the opposite trend developed when aluminum content was above 0.04 wt-%.

In 1992, G. M. Evans (Ref. 6) reported the effect of aluminum on the microstructure and properties of all-weld-metal C-Mn steel weld deposits. The E7018-type weld metals used had aluminum content ranging from 0 to 610 ppm at the heat input of 1 kJ/mm. The average inclusion sizes for all weld metals were found to be between 0.32 and 0.38 mm. The volume fraction of acicular ferrite generally decreased with increasing aluminum content in the weld metals, which agreed with Brownlee's above conclusion. In a weld thermal cycle, the residence time of a SMA weld at temperatures higher than 1000°C is generally less than that for a SA weld. Consequently, the growth of inclusion particles in a SMA weld metal is expected to be much less, resulting in smaller inclusions. That may be the reason why Evans (Ref. 6) observed only a narrow range of inclusion size distribution. Small inclusions were expected to pin the austenite grain boundary movement to result in finer prior austenite grains that promote the formation of grain boundary ferrite. As a result, less intragranular volume of austenite would be left for acicular ferrite nucleation and growth. Especially in the case of SMA weld metals, increasing the aluminum content resulted in less oxygen for titanium and manganese to form oxides such as $TiO_2 \bullet MnO$ and $MnO \bullet Al_2O_3$ (galaxite), which have been reported to promote the acicular ferrite formation (Ref. 6). Therefore, the volume fraction of acicular ferrite decreases with increasing aluminum content in the weld metals.

Effect of Titanium and Its Interaction with Mn, B, O, and N

In 1985, Snyder (Ref. 7) investigated the effect of Ti on SA weld metals. He concluded that for C-Mn steel weld metals, ferrite veining (*i.e.*, well-developed grain boundary ferrite) occurred and toughness deteriorated with increasing titanium content from 100 to 900 ppm.

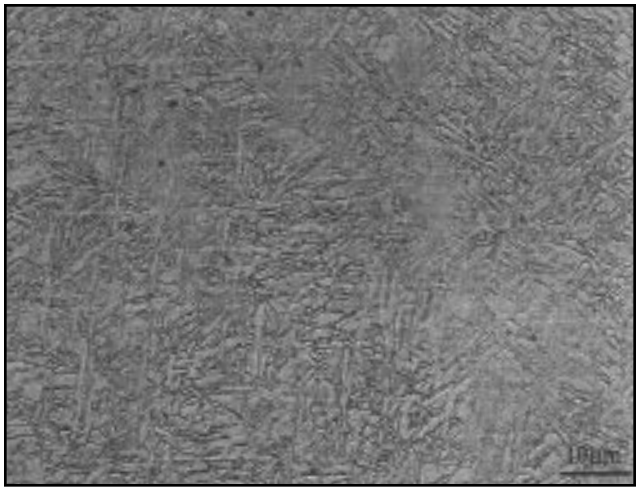

Fig. 5 — Morphology of FS(A) phase under light microscope.

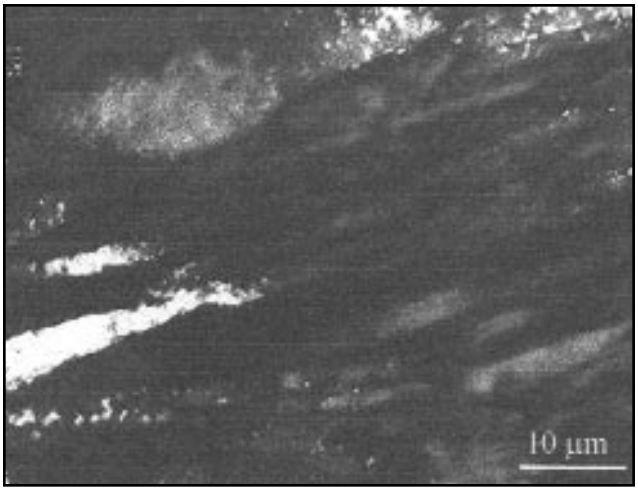

Fig. 6 — TEM morphology of FS(A) phase.

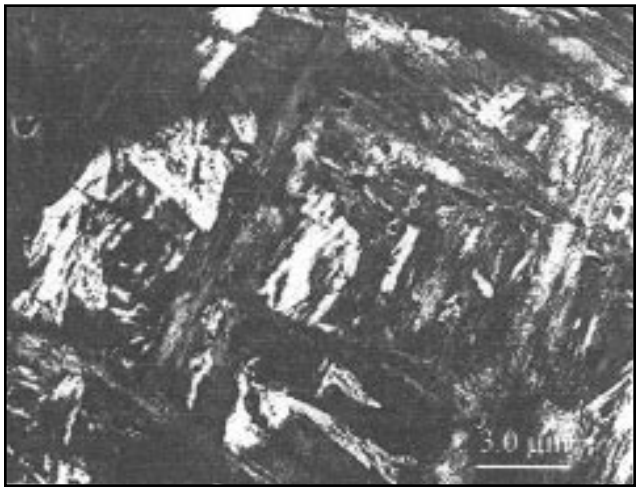

Fig. 7 — TEM morphology of acicular ferrite.

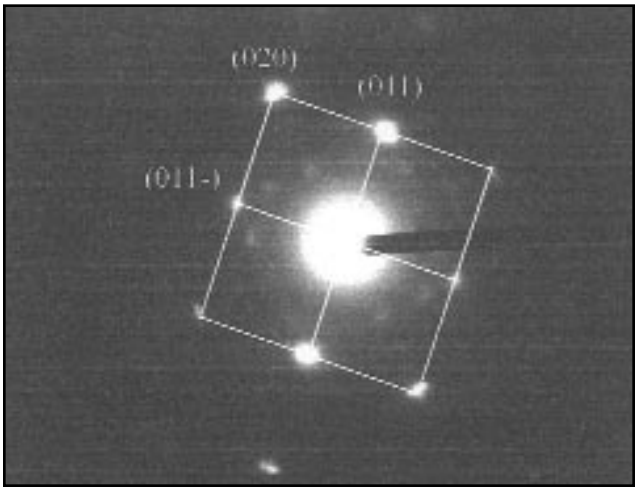

Fig. 8 — Electron diffraction pattern of the dispersed phase in weld C that resembles that of α-ferrite.

However, titanium at a level of 90 ppm could substantially increase toughness. On the other hand, Evans (Ref. 8) closely examined the effect of Ti ranging from 6 to 255 ppm on C-Mn steel weld metals. He found a substantial increase in the volume fraction of acicular ferrite around 22 ppm of Ti, at the expense of ferrite with second phase (FS) in weld metals. Two titanium contents, 30 and 200 ppm, were found to result in high weld metal impact toughness properties.

In spite of the titanium effect, Snyder (Ref. 7) also reported an improvement in toughness by introducing 0.5 wt-% Mo or 0.42 wt-% Mo and 0.84 wt-% Ni in his weld metals. It was found the amount of ferrite veining decreased while acicular ferrite increased by the addition of those alloying elements. In 1996, Johnson (Ref. 9) systematically changed Ti content from 7 to 1000 ppm while keeping about 3.35 wt-% Ni and 0.46 wt-% Mo unchanged in his weld metals. His finding of the titanium effect generally agreed with that of Evans (Ref. 8). In addition, Johnson identified another acicular ferrite volume-fraction peak at 560 ppm titanium in the weld metals. All inclusions in these welds had diameters greater than 0.5 mm. Aluminum content was lower than 150 ppm; however, oxygen content was above 500 ppm. Therefore, the [Al wt-%]/[O wt-%] ratio was 0.3 which, according to Brownlee's criterion (Ref. 5), would result in high amounts of acicular ferrite. This behavior was indeed confirmed in Johnson's weld metals.

Not only does titanium have a strong influence on microstructural evolution and development of mechanical properties in HSLA steel weld metal, it also exhibits a strong interaction with other alloying elements. Snyder (Ref. 7) observed the combination of high manganese and low titanium could improve impact toughness by suppressing formation of ferrite veining. As such, the effects of Ti-N and Ti-B inclusions were also investigated (Refs. 10–15).

In 1997, Liu and Liao (Ref. 10) reported TiN would resist coarsening and dissolution even at temperatures over 1350°C and would more effectively retard austenite grain growth during welding thermal cycles. Due to the TiN effect, the coarse-grained heat-affected zone (CGHAZ) of the high-nitrogen steel (130 ppm N) exhibited fine austenite grains and an adequate amount of grain boundary ferrite while offering zigzag cracking paths along the grain boundaries instead of the transgranular fracture as in the low

Table 1 — Systematic Studies of the Influence of Copper on Weld Metal Toughness (Ref. 23)

Author (Year)	Weld Method	Heat Treatment	Copper Contents	Nickel Levels	Copper Source	Cu (wt-%)
Vidts and de sy (1970)	SAW	Normalized	nil to 1.3%			Optimum toughness at 0.9%
Heuschkel (1973)	GMAW	AW	0 to 0.85%		wire	Copper increases both yield strength and toughness of weld metal
Shackleton (1973)	GMAW	600°C, 10 h	0.07 and 1.12% for Ni free. 0.09 Ni and 1.43% for Ni-alloyed weld metal	0 and 2% Ni	melt-in	More than 1% makes the weld metal somewhat less ductile than 0.07% Cu
Widgery (1978)	GMAW 1.9 kJ/mm	AW	0.28, 0.43, 0.52, 0.86%	Ni/Cu 0/0, 1/2, 1/1, 2/1	wire	Very small influence of copper on toughness
Borisenko, et al. (1976)	GMAW 1.7 kJ/mm	AW	0.3 to 1%	0 and 0.70% Ni	base metal of different Cu content	Optimum toughness at 0.45% Cu
Easterling, et al. (1972)	MMA	AW	0.02, 0.62, 1.06%		electrode	Best toughness at 0.62% Cu
Hannerz (1972)	SAW	AW	nil to 0.4%		wire	Toughness improves with rising copper content up to 0.40% Cu
Hannerz (1983)	SAW	AW and AW +590°C, 1 h	nil to 1.3%	0 and 0.70% Ni	base metal	Optimum in stress-relieved condition at 0.4 for Ni-alloyed and 0.6% for nickel-free weld metal. Optimum at 0.6% Cu for as-welded, Ni-free weld metal.
Fenn and Roberts (1983)	SAW 5.6 kJ/mm	AW	0.18, 0.27, 0.42, 0.68%		melt-in	No influence on 50% fracture surface transition up to 0.42%. Upper shelf levels with rising copper content.
Debiez (1985)	GMAW 1.5, 2.5 kJ/mm	AW and AW +600°, 30 min	1.5 kJ/mm 0.03,0.17, 0.47, 0.97, 1.37%; 2.5 kJ/mm 0.04, 0.15, 0.59, 1.16, 1.30%		same wire, plates with different Cu %	Upper shelf level drops at 1% Cu. Further drop in toughness at higher content. Determined influence of stress relieving at 1% Cu or more.

nitrogen steel (~30 ppm N). As for Charpy V-notch impact testing, the increase of the cracking path resulted in greater absorption of energy to improve the impact toughness.

The interaction of Ti and B and its effects were also investigated. Mori, *et al.* (Ref. 11), proposed that boron atoms along the weld metal austenite grain boundaries retarded nucleation of proeutectoid ferrite while providing favorable conditions for acicular ferrite nucleation. Titanium served to protect the boron from oxygen and nitrogen. Recently, Evans (Ref. 12) found the maximum amount of acicular ferrite occurred at lower B content, around 25–50 ppm, for different Ti levels. From the viewpoint of impact toughness (Ref. 12), the optimal combination of the two elements was 400 ppm Ti and 40 ppm B. Similar ranges of Ti and B additions had been reported earlier by Oh and Olson (Ref. 13). They also indicated that in place of Ti, Zr was also effective with B in maximizing acicular ferrite formation. In underwater wet welding, Ti and B were also found to exhibit an optimal combination range to maximize acicular ferrite formation (Ref. 14). However, as reported by Sanchez and Liu (Ref. 14), this range is shifted to 200 ppm Ti and 20 ppm B. The presence of nitrogen in Ti-B weld metal was detrimental to toughness (Ref. 15). Evans reported a strong fluctuation of the microstructure distribution due to the nitrogen effect. That mechanism needs further exploration.

Effect of Chromium, Molybdenum, and Their Interactions with Manganese

Chromium and molybdenum are similar in terms of their effects on C-Mn steel weld metals. Evans (Refs. 16, 17) reported their effects on the microstructure of C-Mn welds with 1 wt-% Mn. Maximum acicular ferrite was achieved by 0.5 wt-% Mo or 1.1 wt-% Cr additions separately. However, it was found the best impact toughness happened at lower than 0.5 wt-% Mo or 1.1 wt-% Cr. Evans's works showed impact toughness of weld metals with Cr additions increased with Mn content. Furthermore, the toughness of weld metals with Mo additions increased with Mn to a certain point and

Table 2 — Chemical Compositions (in wt-%) of ¾-in.-thick HSLA-100 Base Metals Used

	Steel A[a]	Steel B[b]
C	0.082	0.072
S	0.005	0.005
P	0.010	0.009
Si	0.35	0.23
Cr	0.60	0.10
Ni	3.30	1.63
Mn	0.77	1.33
Cu	1.27	0.93
Mo	0.65	0.20
Nb	<0.01	0.049
Ti	0.01	0.015
Al	0.032	0.026
Fe	Balance	Balance

(a) U.S. manufacturer.
(b) Japanese manufacturer.

Table 3 — Target Chemical Compositions (in wt-%) of HSLA-100 Steel Weld Metals Designed in the First Iteration

Element	wt-%
C	0.08
Mn	1.2
Si	0.28
P	0.007
S	0.003
Ni	3.0
Cr	0.68
Mo	0.50
Cu	(see below)
Nb	(see below)
Fe	balance

Single-Pass Welding with 1.0 kJ/mm Heat Input

Designation	A	B	C	D
Cu	0.0	2.5	3.2	3.7

Multipass Welding with 1.0 kJ/mm Heat Input

Designation	A1-1	B1-1	C1-1	D1-1	B1-Nb
Cu	0.0	2.5	3.2	3.7	2.5
Nb	—	—	—	—	0.03

then decreased with further increases in Mn content. When 1.0 wt-% Mo was added to the weld metal, the Mn content corresponding to the best impact toughness shifted from 1.4 wt-% (without Mo) to 1.1 wt-% (with Mo). In general, Mo has a stronger detrimental effect than Cr regarding toughness.

Effect of Nickel and Its Interaction with Manganese

Nickel has been suggested as beneficial to the toughness of weld metals for a long time. However, it has recently been recognized the benefit from nickel is conditional. In 1991, Evans (Ref. 18) reported that, at low manganese content of usually less than 1.0 wt-%, increasing nickel in weld metal could progressively increase the volume fraction of acicular ferrite in a C-Mn weld metal. However, when manganese content was high, the acicular ferrite would progressively be consumed by martensite and ferrite in the form of ferrite with second phase aligned (FS(A)). It was also reported when the manganese content was about 1.4 wt-%, typically regarded as the optimal level for a C-Mn steel weld metal, toughness dropped when the nickel content exceeded 2.25 wt-%. In addition, Evans's results (Ref. 16) agreed closely with the findings of Zhang, *et al.* (Ref. 19), in 1997. Zhang showed the best toughness was achieved with a high volume fraction of acicular ferrite (>60%), instead of the highest (>80%). Therefore, an optimal weld metal microstructure requires high acicular ferrite but not the highest level of acicular ferrite content. Achieving a high enough proportion of acicular ferrite and ensuring the least amount of martensite would result in good toughness. In addition, high nickel contents tend to promote microsegregation of Ni, Mn, and Si in networks or parallel to grain boundaries in low-temperature reheated zones (<900°C), leading to the reduction of toughness (Ref. 19).

Copper Precipitation Effect in Multipass Weld Metals

As a precipitation agent, copper has a strong effect on strengthening, microstructural evolution, and toughness of HSLA steel weld metals. Es-Souni, *et al.* (Ref. 20), introduced different levels of copper content, ranging from 0.0 to 3.2 wt-%, into a SMAW electrode coating designed for plain carbon steel welding. He noticed a solid-solution strengthening effect at a copper content of up to 0.19 wt-%. When copper content increased above 0.66 wt-%, copper precipitation strengthening was evident. In addition, he also found copper preferentially precipitated along dislocations and interphase boundaries, which agreed with Thompson's observation (Ref. 21). Based upon quantitative metallography, Es-Souni showed the volume fraction of FS(A) increased with copper content. Based on tensile and Charpy V-notch impact data, he concluded 0.66 wt-% copper content was desirable for both strength and toughness of plain carbon steel weld metals. However, Krishnadev, *et al.* (Ref. 22), explored lower levels of copper content, ranging from 0.046 to 0.56 wt-%, in HSLA-100 steel weld metals that contained Ni, Cr, and Mo, and obtained a higher strength level (greater than 100 ksi (690 MPa)) and fair Charpy V-notch toughness (40.6 ft-lb (55 J) at –51°C (–60°F)). Good mechanical properties led to the conclusion 0.5 wt-% copper content in the weld metal did not cause any adverse effect on toughness.

Other researchers have also discussed the beneficial addition of copper in weld metal at different welding conditions. Hannerz summarized the major conclusions of these researchers in Table 1 (Ref. 23). No agreement on optimal copper contents in steel weld metals could be reached.

Based on the effects of the alloying elements discussed above and the chemical composition of steels A and B (Table 2) collectively, it was decided the content of alloying elements in HSLA-100 steel weld metal must be initially designed to be no greater than those in the base metal to avoid overhardening and to leave enough opportunities for later optimization of the alloying system. Based upon the metallurgical and mechanical performance of resultant welds, stepwise optimization of the alloying system would be carried out to achieve the goal of this work of designing a SMAW electrode for HSLA-100 steel with a 100 ksi (690 MPa) level yield strength and no less than 65, 45, and 35 ft-lb (87, 60, and 47 J) Charpy V-notch impact toughness at 0, –40, and –60°F (–18, –40, and –51°C).

Experimental Procedures

Two types of HSLA-100 steel plates were used in this investigation. Their designations and chemical compositions are listed in Table 2. Welding electrodes with 5/32-in. diameters were designed and man-

Table 4 — Target Chemical Compositions (in wt-%) of Experimental HSLA-100 Steel Weld Metals Designed in the Second Iteration

Element	wt-%
C	0.05
Mn	1.2
Si	0.28
P	0.007
S	0.003
Ni	(see below)
Cr	0.0
Mo	0.50
Ti	240–400 ppm
N	max 100 ppm
O	max 250 ppm
Cu	(see below)
Nb	0.03
Fe	balance

Multipass Welding with 1.0 kJ/mm

Designation	A2-1	B2-1	C2-1	D2-1	E2-1
Cu	1.0	1.5	1.5	1.0	1.5
Ni	3.0	3.0	1.0	2.0	2.0

Multipass Welding with 2.0 kJ/mm

Designation	A2-2	B2-2	C2-2	D2-2	E2-2
Cu	1.0	1.5	1.5	1.0	1.5
Ni	3.0	3.0	1.0	2.0	2.0

ufactured in three iterations. The first iteration of electrodes had four different levels of copper ranging from 0.0 to 3.7 wt-%. Detailed weld metal target compositions and weld metal designations are listed in Table 3. In the second iteration, chromium was removed and the Ni and Cu contents were adjusted to 1.0–3.0 and 1.0–1.5 wt-%, respectively. In addition, niobium content was controlled at 0.03 wt-% (Table 4). Finally, the electrodes in the third iteration further lowered the carbon content to 0.03 wt-% and the nitrogen content to 100 ppm maximum. The nickel and copper contents were fine-tuned to 1.0–2.3 and 0.8–1.0 wt-%, respectively. The contents of all other alloying elements of the third-iteration electrodes are reported in Table 5.

Single-pass, bead-on-plate welding and multipass welding were both performed on steel A in the flat position and at 1.0 and 2.0 kJ/mm heat input. The multipass welding was made on a single-V-groove plate with a 20-deg included angle and a ⅝-in. root opening. Plate thickness was ¾ in. Nine layers and 31 passes were used to fill in the groove at 1.0 kJ/mm; while seven layers and 16 passes were used for the 2.0 kJ/mm heat input. The joint surface was buttered to eliminate the dilution effect from the base metal. For the welds made using the first-iteration electrodes, welding voltage was 22.5 V and welding current was 155 A. A Hobart Cyber-TIG 300 series power source, direct current, electrode positive (DCEP) was used. Interpass temperature was controlled to be 300°F (~150°C) and preheating temperature was about 77°F (25°C).

Weld metals using second- and third-iteration electrodes were produced using steel B plates by The Lincoln Electric Co. Welding voltage and current were 22.5 V and 170 A, respectively. The interpass temperature was 300°F (150°C) for the 1.0 kJ/mm welding and 325°F (163°C) for the 2.0 kJ/mm welding with 300°F (150°C) preheating. Other welding conditions were the same as those in the first iteration.

Complete chemical analysis on all weld metals was performed prior to mechanical tests, which included tensile and Charpy V-notch impact tests. All-weld-metal tensile specimens with 0.5-in. reduced-section diameter were extracted from multipass weld metals along the longitudinal axis of the weld beads (per ASTM E8). All tensile test data were digitally recorded using a personal computer. Standard full-size Charpy V-notch impact specimens were prepared per ASTM E23 from the middle of weld transverse sections with notches perpendicular to the weld axis and tested mainly at –60, –30, and 0°F (–51, –34, and –18°C). Three to five Charpy specimens were broken at each temperature. For selected welds, additional specimens were tested at temperatures of –90°F (–68°C), –70°F (–57°C), and room temperature. In addition, a hardness survey was performed according to the following procedure.

In brief, specimens were extracted from the mid-length of each single-pass weld metal and polished to 0.05-μm finish. A Leco M-400A hardness tester was used to measure the hardness on the weld transverse cross section. A specially designed hardness survey grid was followed (illustrated in Fig. 1). After averaging the hardness from all grid points, the grid point with the hardness closest to the averaged hardness was selected as the "representative" location for the cross section of weld metal in terms of hardness and microstructure. After careful examination of multiple fields, it was concluded the grid points 2 mm off the center (Fig. 1) of the single-pass weld metals were the representative location. For multipass weld metals, a hardness traverse across the weld was performed at the mid-thickness of the weld metals to determine an average hardness for each. The location in the central bead with hardness reading closest to the averaged hardness was chosen as the representative location for each multipass weld. Again, this experimental procedure was adopted after carefully examining multiple fields of weld metal microstructures.

To explore the microstructural evolution, TEM samples extracted from the single-pass weld metal C were prepared for further examination of the different microstructural constituents observed under the light microscope. A Philips EM 400 microscope was used for the TEM examination. Electron diffraction patterns from different phases were recorded and analyzed. After characterizing and identifying the microstructures under the

Table 5 — Target Chemical Compositions (in wt-%) of Experimental HSLA-100 Steel Weld Metal Designed in the Third Iteration

Element	wt-%
C	0.03
Mn	1.25
Si	0.28
P	0.007
S	0.003
Ni	(see below)
Cr	0.0
Mo	(see below)
Ti	240–400 ppm
N	max 100 ppm
O	max 250 ppm
Cu	(see below)
Nb	0.03
Fe	balance

Multipass Welding with 1.0 kJ/mm Heat Input

Designation	A3-1	B3-1	C3-1
Ni	2.2	1.5	1.0
Cu	0.8	1.0	1.0
Mo	0.5	0.25	0.25

Multipass Welding with 2.0 kJ/mm Heat Input

Designation	A3-2	B3-2	C3-2
Ni	2.2	1.5	1.0
Cu	0.8	1.0	1.0
Mo	0.5	0.25	0.25

Table 6 — Chemical Compositions (in wt-%) of Single-Pass Weld Metals Made from Steel A at a Heat Input of 1.0 kJ/mm

Weld	C	S	P	Si	Cr	Ni	Mn	Cu	Mo
A	0.062	0.004	0.008	0.29	0.55	2.98	0.97	1.5	0.47
B	0.060	0.004	0.008	0.26	0.55	2.96	0.95	2.2	0.46
C	0.059	0.004	0.008	0.32	0.55	2.96	1.08	2.55	0.46
D	0.061	0.004	0.008	0.31	0.57	2.99	1.05	2.67	0.47

Table 7 — Results of Quantification Metallography of Single-Pass Weld Metals Made from Steel A at a Heat Input of 1.0 kJ/mm

Weld	GF	FS(A)	AF	M	FS	GB	Hv-500
A	2.3	14.2	55	3.4	3.1	22	328
B	0.5	17	35.8	10.8	10.2	25.6	370
C	0.5	37	21	12	7.5	32.5	371
D	2.9	30.9	40.5	7.7	0.6	17.3	347

GF = grain boundary ferrite; FS(A) = ferrite with second phase aligned; AF = acicular ferrite; M = martensite; FS = ferritewith second phase; GB = granular bainite.

TEM, micrographs were taken at representative locations of the single- and multipass welds made by 1.0 kJ/mm heat input at 1000X magnification for quantitative metallography.

Results and Discussion

Iteration 1

Since microstructural distribution of HSLA-100 steel weld metal depends upon the alloying elements, the chemical compositions of single-pass weld metals (the first iteration) were examined and reported in Table 6. Basically, all alloying elements were maintained at their expected levels except for copper, which ranged from 1.5 to 2.7 wt-% and narrower than the proposed 0.0–3.7 wt-% range. With the level of alloying elements found in the weld metals, a mixed microstructure with grain boundary ferrite (GBF), acicular ferrite (AF), ferrite with second phase aligned (FS(A)), and martensite (M) was expected. A typical micrograph of an HSLA-100 steel weld metal is shown in Fig. 2. Because of the low carbon content, acicular ferrite, ferrite with second phase aligned, and martensite all appeared acicular under a light microscope. Due to their similarity, a careful study was conducted to characterize each individually. Additionally, as illustrated in Fig. 2, there is often a "dispersed" phase in the welds that cannot be categorically characterized as one of the earlier listed phases present in the micrograph. Those microstructural phases were investigated using TEM and the results are summarized as follows:

For lath martensite at low magnifica-

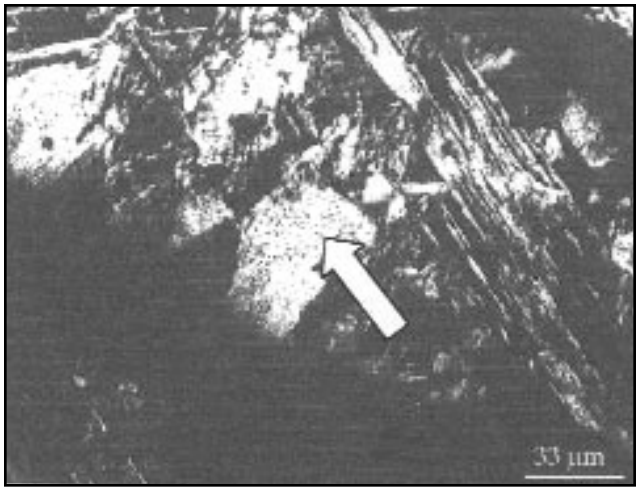

Fig. 9 — TEM micrograph of the dispersed phase indicating a large population of small dots (islands).

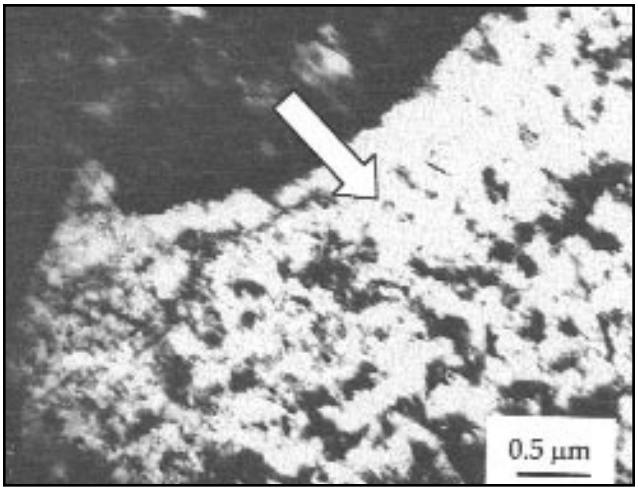

Fig. 10 — Bright-field TEM image of the dispersed phase in weld.

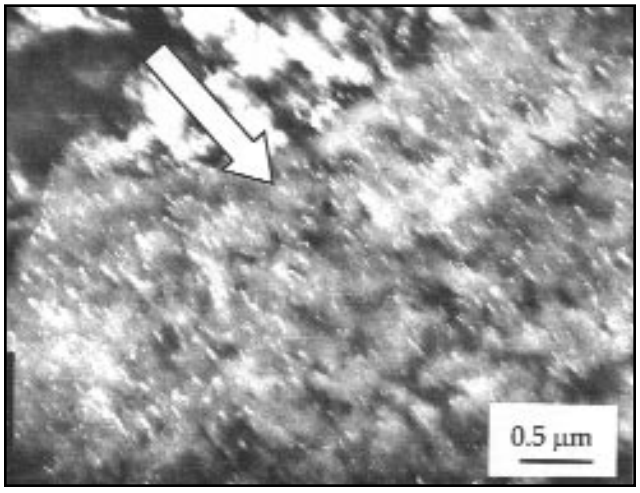

Fig. 11 — Dark-field image of the dispersive phase in weld C with the islands of retained austenite illuminated.

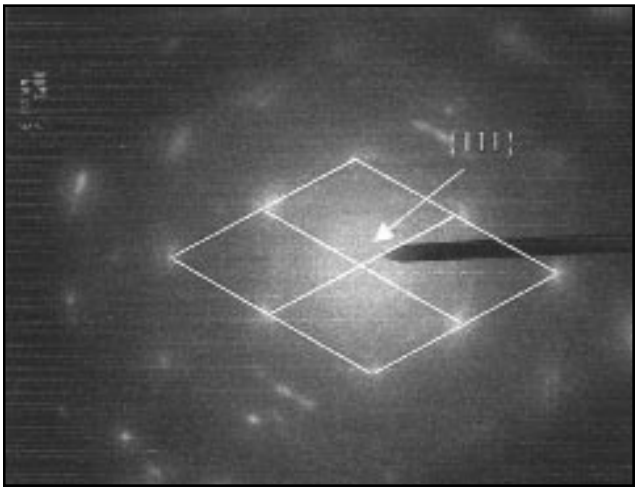

Fig. 12 — The electron diffraction pattern of dark laths in the dispersed phase in weld C.

tion (1000X), they often featured triangular packets — Fig. 3. At higher magnification under an electron microscope (15 kX), a single lath, observed under low magnifications, actually consisted of an array of parallel sublaths — Fig. 4. In addition, the angle between two intersecting "single" laths was approximately 60 deg. This spatial distribution illustrated the triangular feature mentioned before.

The FS(A) laths appear at low magnifications as groups of elongated grains, aligned in parallel — Fig. 5. Each single lath also presented several smaller parallel sublaths at a higher magnification (15 kX) — Fig. 6. The difference between lath martensite and FS(A) is that at light microscope resolution, martensite laths often arrange themselves in triangular packets, while FS(A) laths only organize in parallel packets.

For acicular ferrite, refined laths can be easily identified according to their randomly oriented laths and colonies. However, coarse acicular ferrite laths could be confused with FS(A) laths at low magnification (1000X) under a light microscope in Fig. 2. At higher magnifications under an electron microscope, the differences between a coarse acicular ferrite lath and a FS(A) lath were clear: coarse acicular ferrite laths have no sublaths as appeared in FS(A) laths. The laths of the coarse acicular ferrite often present a 90-deg interlocking pattern (Fig. 7), which was another distinctive feature different from the FS(A) laths.

The electron diffraction pattern of the "dispersed" phase resembled that of α-ferrite — Fig. 8. After further examination of this phase at 15-kX magnification, a population of dark dots (small islands) was observed — Fig. 9. These islands were again examined at a magnification of 25 kX in bright and dark fields — Figs. 10, 11. In the dark field, the large population of tiny white islands could be identified as retained austenite using electron diffraction techniques — Fig. 12. Thus, the "dispersed" phase was actually an α-ferrite-type matrix with retained austenite islands. Since low-carbon martensite crystal has an electron diffraction pattern basically the same as that of ferrite and no cementite was found, the dispersed phase fits the description of granular bainite, which was first reported by Habraken and Economopous (Ref. 24) and more recently reexamined by Thompson (Ref. 25). Therefore, the dispersed phase found in this study was classified as granular bainite (GB).

After knowing the morphological

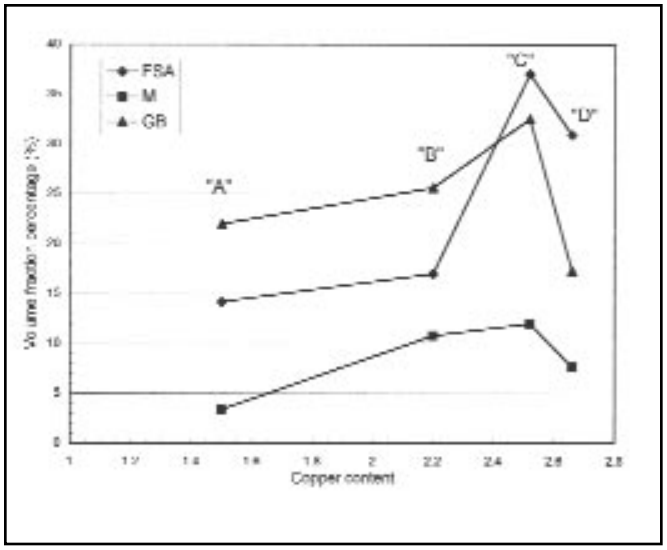

Fig. 13 — Effect of microstructures on the hardness of a HSLA-100 A weldment.

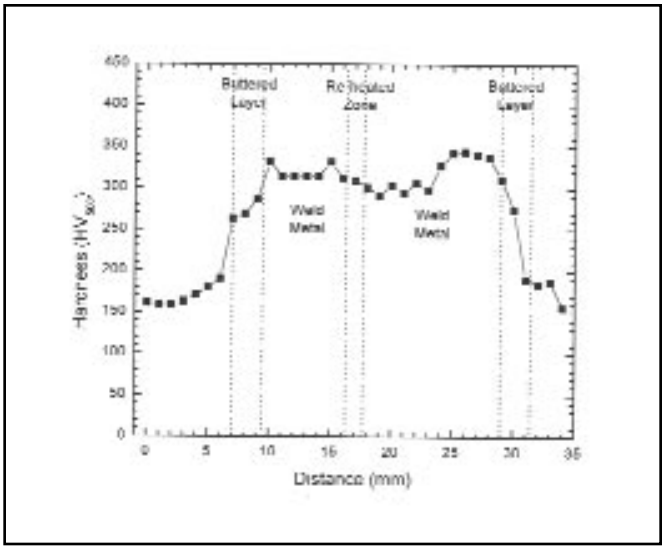

Fig. 14 — Hardness survey on the cross section of multipass E2-1 weld metal with 0.03 wt-% Nb addition.

Table 8 — Chemical Compositions (in wt-%) of Multipass Weld Metals Made at 1.0 kJ/mm in the First Iteration

Weld	A1-1	B1-1	C1-1	D1-1	B1-Nb
C	0.09	0.080	0.10	0.08	0.09
S	0.009	0.010	0.011	0.010	0.011
P	0.010	0.011	0.012	0.011	0.011
Si	0.42	0.41	0.42	0.40	0.46
Cr	0.72	0.72	0.77	0.74	0.73
Ni	3.26	3.21	3.42	3.29	3.16
Mn	1.40	1.37	1.51	1.43	1.49
Cu	0.18	1.96	2.47	2.51	1.96
Mo	0.50	0.52	0.54	0.52	0.50
Nb	0.01	0.01	0.02	0.02	0.05
Ti	110 ppm	100 ppm	150 ppm	200 ppm	570 ppm

Table 9 — Microstructural Quantification Results of Multipass Weld Metals Made at 1.0 kJ/mm in the First Iteration

Phases	Retained Austenite	FS(A)	AF	Lath M	FS	GB
A1-1	1.7	28.4	12.5	0	41.5	15.9
B1-1	1.0	65.3	9.1	0.6	8.0	16.5
C1-1	2.0	64.2	6.25	0.5	17.6	10.2
D1-1	1.0	76.7	10.2	0.5	4.5	7.4
B1-Nb	0.0	37.5	34.0	1.1	8.5	18.7

characteristics of the microstructural constituents in those HSLA-100 weld metals, quantitative metallography was conducted on single-pass weld metals A through D. The results are shown in Table 7 and Fig. 13. Note the amounts of FS(A), granular bainite, and lath martensite all increased from A to C, then dropped at D. This interesting profile of microstructural evolution corresponded well with the hardness change (Table 7). Increasing copper up to about 2.5 wt-% appeared to promote formation of FS(A), M, and GB.

Furthermore, it is important to verify this trend for multipass weld metals. After multipass welding, the chemical compositions of those weld metals were examined and the results listed in Table 8. It can be seen from A1-1 to D1-1, only the copper content progressively increased while the other contents remained reasonably constant. This pattern of copper increase is similar to that of single-pass welds. Note a small amount of Nb was introduced into B1-1 alloying system to result in the B1-Nb weld metal. This addition was based on the findings of Ramirez and Liu (Ref. 26) of synergistic precipitation of Cu/Nb in HY130 steel weld metals. The microstructures were quantified in Table 9 and their mechanical properties presented in Table 10. It is obvious the amount of FS(A) phase progressively increased from A1-1 to D1-1 by consuming AF, FS, and GB phases. The general change of the FS(A) amount with respect to copper was in phase with the change in yield strength and ultimate tensile strength and out of phase with the change

Table 10 — Mechanical Properties of the Multipass Weld Metals Obtained from the First Iteration

1.0 kJ/mm	A1-1	B1-1	C1-1	D1-1	B1-Nb
Hardness					
Hv-500	279	275	376	286	316
Strength (ksi)					
σ_y	100	115	122	130	132
σ_{UTS}	128	145	153	156	152
elongation	17%	19%	18%	16%	20%
Toughness (ft-lb)					
@ –30°F	43	30	27	24	24
@ 0°F	44	30	28	26	25

Table 11 — Chemical Compositions (in wt-%) for Multipass Weld Metals in the Second Iteration made at 1.0 kJ/mm

Weldment	A2-1	B2-1	C2-1	D2-1	E2-1
C	0.053	0.056	0.056	0.06	0.056
Mn	1.38	1.37	1.32	1.46	1.40
Cu	1.02	1.60	1.53	1.12	1.70
Ni	3.01	2.98	1.15	2.21	2.21
Mo	0.52	0.51	0.56	0.57	0.55
Ti	280 ppm	340 ppm	320 ppm	310 ppm	350 ppm
N	230 ppm	160 ppm	170 ppm	160 ppm	160 ppm
Si	0.34	0.31	0.34	0.33	0.33
O	310 ppm	340 ppm	310 ppm	260 ppm	310 ppm
P	0.014	0.013	0.015	0.015	0.014
S	0.006	0.007	0.007	0.006	0.006
V	0.010	0.010	0.009	0.010	0.010
Cr	0.04	0.05	0.05	0.05	0.04
NB	0.03	0.03	0.03	0.03	0.03

in the Charpy V-notch impact toughness. The correspondence between the mechanical properties and microstructures was again verified. This evidence strongly supports that the hard FS(A) phase change was in sync with the change in strength. On the other hand, it is interesting to observe the amount of AF was significantly increased after adding Nb in the weld metal B1-Nb (almost four times more than the amount in weld metal B1-1). According to Ramirez, *et al.* (Ref. 26), introducing a small amount of Nb in weld metal can substantially increase dislocation density, which provides more random sites for copper precipitation. Much copper precipitation out of the iron matrix results in the decrease of weld metal hardenability. As such, the amount of FS(A) was reduced. This explanation can also be used to justify the trend shown in Fig. 13 for copper content greater than 2.6 wt-%. Even though the toughness of weld metal B1-Nb was not drastically improved, the increase of AF and the suppression of FS(A) were substantial. The reduction of FS(A) phase tended to result in better Charpy V-notch impact toughness. The increase of AF in B1-Nb also shows a promising trend for toughness improvement.

Results of the iteration 1 welds clearly showed the microstructures in A1-1 to D1-1 weld metals were not ideal for achieving a maximum impact toughness, with only about 10% AF, but high FS(A) (more than 50% when copper content was above 1.96 wt-%). With the relatively high amount of FS(A) phase, it is not surprising to overshoot the yield strength to levels higher than 100 ksi. Considering the impact toughness, a decrease in strength is necessary to promote an increase in toughness. Thus, contents of hardening alloying elements must be revised for iteration 2 electrodes.

Iteration 2

Among all the alloying elements in weld metals, Cr and Mo are considered strong hardening agents. However, Mo has an effect of reducing the size of martensite packets (Ref. 27), which benefits toughness. Thus, Cr would be eliminated from the alloying system. In addition to chromium removal, the addition of Ti should be optimized since titanium was reported to be beneficial in promoting formation of AF (Ref. 8). Other than Mo, Cr, and Ti additions, many researchers (Ref. 23) recommended less than 2.0 wt-% copper in HSLA weld metals. Therefore, copper content was targeted to be less than 1.5 wt-%. Since the metallurgical behavior of Ni and Cu is similar, to a certain extent, high Ni content in higher strength HSLA steel weld metals may degrade the toughness level, possibly due to its segregation at interphase regions or grain boundaries (Ref. 19). Therefore, nickel content should be adjusted in conjunction with copper. Finally, more effort would be made to further decrease carbon content in HSLA-100 steel weld metal.

Based on the above considerations, new alloy systems designed for the second iteration work are shown in Table 4. The resultant chemical compositions of weld metals agreed well with the designed values (Table 11) except for the high nitrogen content. The unexpected nitrogen content might have come from nitrogen-contaminated Fe-Ti or Ti powder. The work to reduce the nitrogen content was left for the third iteration. Results of tensile and impact tests are listed in Table 12.

Quantitative metallography results for weld metals made by 1.0 kJ/mm heat input are listed in Table 13. By decreasing nickel content from 3.0 to about 2.2 wt-% while maintaining copper content, *i.e.*, weld metal A2-1 vs. D2-1, and weld metal B2-1 vs. E2-1, the weld metal hardenability was decreased, with partial suppression of the formation of the low-temperature product FS(A). For example, volume fraction of FS(A) was decreased

Table 12 — Mechanical Properties of Multipass Weld Metals Made at 1.0 and 2.0 kJ/mm Heat Inputs in the Second Iteration

1.0 kJ/mm	A2-1	B2-1	C2-1	D2-1	E2-1
Strength (ksi)					
σ_y	—	—	126	121	120
σ_{UTS}	cracked	cracked	127	126	134
elongation	—	—	32.7%	cracked at 1.6%	cracked
Toughness (ft-lb)					
@ –60°F	32	24	43	45	38
@ –30°F	35	31	57	59	48
@ 0°F	30	24	63	59	55
2.0 kJ/mm	A2-2	B2-2	C2-2	D2-2	E2-2
Strength (ksi)					
σ_y	120	117	106	112	120
σ_{UTS}	130	135	112	118	124
elongation	27%	cracked at 5.4%	cracked at 2.0%	31%	cracked at 3.4%
Toughness (ft-lb)					
@ –60°F	47	40	42	56	42
@ –30°F	57	43	55	61	47
@ 0°F	63	45	63	73	53

Table 13 — Quantitative Metallography Results for the Second Iteration of Weld Metals Made at 1.0 kJ/mm

Phases	Retained Austenite	FS(A)	AF	Lath M	FS	G.B.
A2-1	1.7	38	40	0.6	13	6.8
B2-1	1.7	34.6	35.2	9	14.8	10.2
C2-1	0.6	8.0	72.7	0	2.3	16.4
D2-1	0.0	15.9	47.7	1.7	5.1	29.5
E2-1	0.0	29	37.5	1.7	17.7	14.2

from 38% in weld metal A2-1 to 15.9% in weld metal D2-1. On the contrary, volume fraction of AF increased from 40% in weld metal A2-1 to 48% in weld metal D-2. Similar changes in microstructure also happened in weld metals B2-1 and E2-1. The same is true for the GB volume fraction change. As a result, the increase of AF and GB volume fraction improved Charpy V-notch impact toughness in weld metals D2-1 and E2-1. In addition, the increase of volume fractions of AF improved impact toughness as a result of regulating Ni content to about 1.15 wt-% while keeping copper content to about 1.5 wt-% in weld metal C2-1 with 0.03 wt-% Nb and 0.5 wt-% Mo. The weld metal exhibited an improved microstructure with predominantly AF and almost no martensite (Table 13).

The hardness fluctuation (Δ hardness) on cross sections of 1.0 kJ/mm weld metals was also minimized from more than 100 DPH with no Nb addition (Ref. 24), to less than 50 DPH with 0.03 wt-% Nb addition, as shown in Fig. 14. This minimization of hardness fluctuation was attributed to the synergistic precipitation mechanism in the Cu-Nb enhanced weld metals as proposed by Ramirez and Liu (Ref. 26). On the other hand, preexisting cracks were found in several of the all-weld-metal tensile samples. With a bluish, iridescent tinted surface, those defects were concluded as hot cracking. Charpy V-notch impact toughness for several weld metals was unsatisfactory (Table 12). Only weld metal D2-2 made at 2.0 kJ/mm showed some potential for further development to meet the Navy's requirement for the Charpy V-notch impact toughness of HSLA-100 weld metals. For 1.0 kJ/mm weld metals, only C2-1 (1.5 wt-% Cu and 1.2 wt-% Ni) and D2-1 (1.1 wt-% Cu, 2.2 wt-% Ni) weld metals performed close to the Navy's toughness requirement. Profiles of weld metal toughness and yield strength with respect to the Cu content in the welds were plotted in Figs. 15 and 16. It clearly shows two pairs of Cu/Ni contents (see arrows in Fig. 15), *i.e.*, 1.5 wt-% Cu with 1.2 wt-% Ni in weld metals C2-1 and C2-2 and 1.1 wt-% Cu with 2.2 wt-% Ni in weld metals D2-1 and D2-2 resulted in mechanical properties closest to the Navy's requirements. Therefore, they were chosen as candidates for the alloying system optimization of the third iteration.

Iteration 3

Considering weld metals with 1.5 wt-% copper and 1.2 wt-% nickel (weld metal C2-1) and 1.1 wt-% copper and 2.2 wt-% nickel (weld metal D2-1), their yield strengths were still 120 ksi strong. It was the 73% and 48% volume fractions of AF in the corresponding weld metals that propelled their Charpy V-notch impact toughness close to the U.S. Navy's requirement. Because of the high yield strength, there was still some margin of strength for trade-off to achieve a better toughness. High strength implied the contents of Mo and Ni — hardenability elements — could still be fine-tuned to achieve a better microstructural distribution for better toughness. In addition to that, carbon and nitrogen in weld metals also needed to be further reduced. The targeted alloying systems were already presented in Table 5.

Welding, mechanical testing, and microstructure examination were again conducted for the third iteration of the work. Chemical compositions for weld metals made by 1.0 and 2.0 kJ/mm heat inputs were listed in Table 14. Results for the mechanical properties were listed in Table 15 and shown in Figs. 17 and 18. Those mechanical properties met the Navy's requirements mentioned before. As can be seen, the molybdenum content was reduced from 0.54 to 0.26 wt-% in welds A3-1 to C3-1, respectively. From the corresponding micrographs shown in Fig. 19A–C, the martensite packet size indeed increased from weld metals A3-1 to

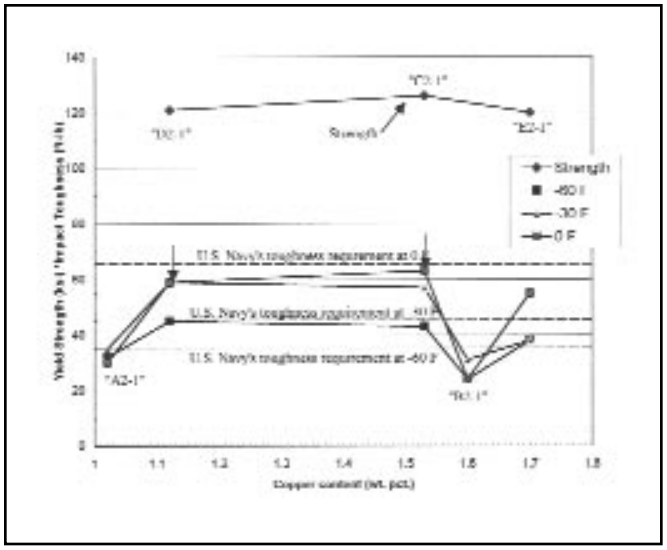

Fig. 15 — Yield strength and toughness performance with respect to the copper content in multipass weldments made at 1.0 kJ/mm heat input in the second iteration.

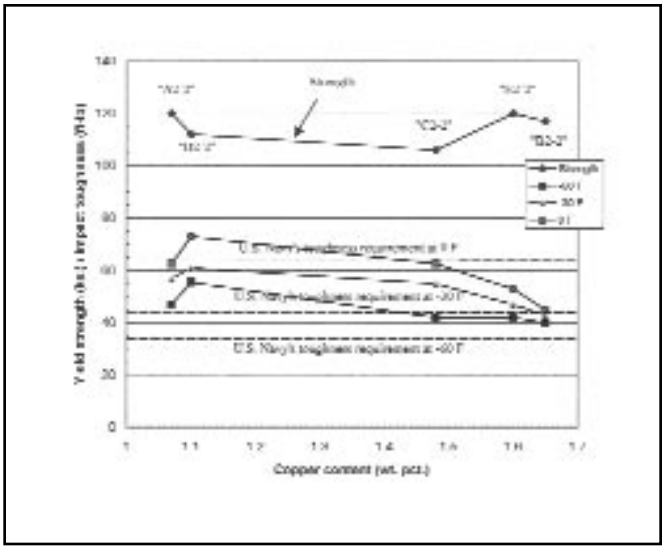

Fig. 16 — Yield strength and toughness performance with respect to the copper content in multipass weldments made at 2.0 kJ/mm heat input in the second iteration.

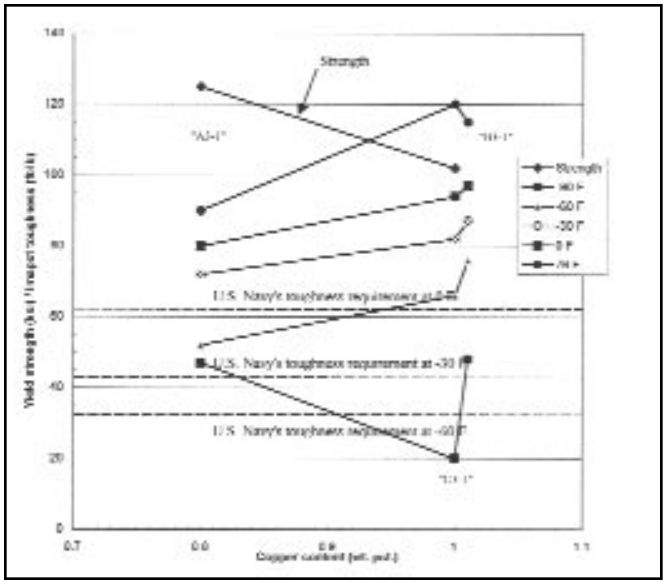

Fig. 17 — Yield strength and toughness performance with respect to the copper content in multipass weldments at 1.0 kJ/mm heat input in the third iteration.

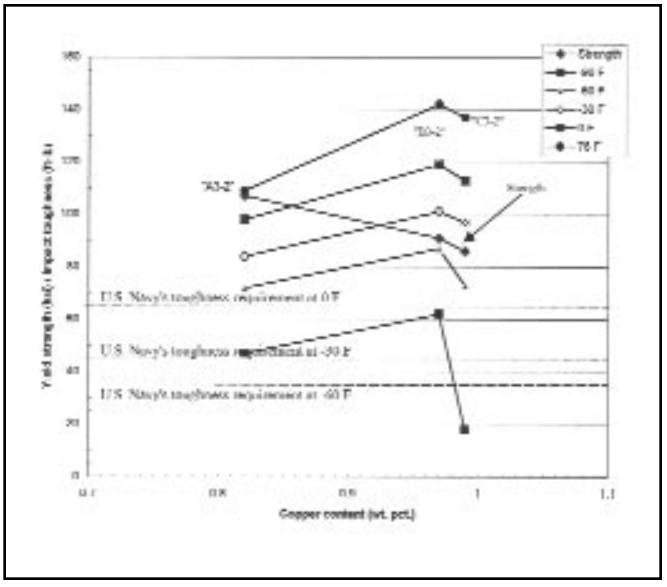

Fig. 18 — Yield strength and toughness performance with respect to the copper content in multipass weldments made at 2.0 heat input in the third iteration

B3-1 (Ref. 25). Since the martensite packet can be treated as a "sub-grain" unit (Ref. 25), increasing the size of the martensite packet resulted in a decrease in strength and hardness, as shown in Table 15. Consequently, toughness was increased from weld metals A3-1 to B3-1 However, with too much increase of the size of martensite packets in weld metal C3-1, the toughness again decreased (from weld metals B3-1 to C3-1). In addition to the molybdenum effect, nickel's effect is also obvious when copper was kept at the level of about 1.0 wt-%. By decreasing nickel content together with that of the Mo content from weld metal A3-1 to C3-1, the amount of grain boundary ferrite was observed to increase and the toughness was slightly decreased from weld metals B3-1 to C3-1. It was also noticed the fine FS(A) laths found in weld metal B3-1 was coarser than those in weld metal A3-1 and ended up with a well-developed grain boundary ferrite in weld metal C3-1. The sequence seems to suggest the microstructure along the grain boundaries experienced an evolution that started with a fine dispersion of FS(A) laths and ended with grain boundary ferrite from weld metals A3-1 to C3-1. The finer FS(A) may be related to both high alloying contents and a sufficient amount of carbides for the interphase precipitation, which led to the lath refinement in weld metal A3-1. Lath coarsening of the FS(A) phase followed because of decreases in both hardenability and the amount of carbide formed in weld metal B3-1 (about 12% lath-coarsened FS(A) was found in the weld metal B3-1). Finally, grain boundary ferrite formed because of further reduction of nickel and

Table 14 — Chemical Compositions (in wt-%) of Multipass Weld Metals Made at 1.0 and 2.0 kJ/mm in the Third Iteration

(1.0 kJ/mm)	A3-1	B3-1	C3-1
C	0.045	0.051	0.047
Mn	1.31	1.35	1.26
Si	0.29	0.30	0.26
Ni	2.30	1.52	1.04
Mo	0.54	0.28	0.26
Ti	230 ppm	240 ppm	220 ppm
N	90 ppm	90 ppm	70 ppm
O	270 ppm	300 ppm	290 ppm
Cu	0.80	1.01	1.00
P	0.012	0.012	0.011
S	0.004	0.005	0.004
V	0.009	0.009	0.008
Cr	0.03	0.03	0.03
Nb	0.03	0.03	0.03
(2.0 kJ/mm)	A3-2	B3-2	C3-2
C	0.045	0.046	0.044
Mn	1.31	1.28	1.18
Si	0.25	0.23	0.21
Ni	2.32	1.51	1.05
Mo	0.55	0.27	0.28
Ti	180 ppm	190 ppm	170 ppm
N	90 ppm	110 ppm	120 ppm
O	270 ppm	270 ppm	290 ppm
Cu	0.82	0.97	0.99
P	0.013	0.012	0.011
S	0.004	0.004	0.005
V	0.009	0.008	0.008
Cr	0.03	0.04	0.03
Nb	0.03	0.03	0.03

Table 15 — Mechanical Properties of the Multipass Weld Metals Made at 1.0 and 2.0 kJ/mm Heat Inputs in the Third Iteration

1.0 kJ/mm	A3-1	B3-1	C3-1
Hardness (Hv-500)	281.5	260	245
Strength (ksi)			
σ_y	125	—	102
σ_{UTS}	129	—	109
elongation	37%	—	47%
Toughness (ft-lb)			
@ –90°F	47	48	20
@ –75°F	—	65	—
@ –60°F	52	76	66
@ –30°F	72	87	82
@ 0°F	80	97	94
@ 76°F	90	115	120
2.0 kJ/mm	A3-2	B3-2	C3-2
Strength (ksi)			
σ_y	107	91	86
σ_{UTS}	116	101	97
elongation	35%	37%	43%
Toughness (ft-lb)			
@ –90°F	47	62	18
@ –75°F	—	68	—
@ –60°F	72	87	73
@ –30°F	84	101	97
@ 0°F	98	119	113
@ 76°F	109	142	137

molybdenum contents in weld metal C3-1. It is reasonable to deduce those fine FS(A) laths cannot effectively resist cracking because of interlath carbide arrays; on the other hand, the coarser FS(A) laths can more effectively reduce the amount of interlath carbide arrays by reducing the total area of the interlath surface. Therefore, the coarse FS(A) structure (relative to the fine FS(A) structure) actually became tougher. Indeed, weld metals B3-1 and B3-2 had the highest toughness, which provided support for the explanation.

In general, all Charpy V-notch impact toughness values were well above the U.S. Navy's requirement. The yield strength of weld metal A3-1 can satisfy the 100-ksi yield strength requirement at both 1.0 and 2.0 kJ/mm heat input. It was successfully developed for the HSLA-100 steel to satisfy the U.S. Navy's mechanical property requirements.

Conclusions

The major conclusions of this research can be summarized as follows:

1. The optimal alloying system for an HSLA-100 steel weld metal can be proposed to be 0.04 wt-% C, 1.3 wt-% Mn, 2.3 wt-% Ni, 0.25–0.55 wt-% Mo, 0.8 wt-% Cu, 90 ppm N, and 270 ppm O.
2. 0.03 wt-% Nb worked well for the Cu/Nb synergistic precipitation to minimize hardness fluctuation on the transverse cross section of the HSLA-100 steel weld metals.
3. The weld metal with a predominant AF microstructure (around 70%) and considerable amount of granular bainite (around 15%) showed respectable impact toughness results for high-strength steels.
4. With the AF and GB optimized, coarse FS(A) appeared to further enhance the toughness performance by offering greater resistance to crack propagation.

Acknowledgments

The authors would like to acknowledge the support of Dr. George Yoder of the U.S. Office of Naval Research. Appreciation also goes to Oerlikon Buhrle Ltd. (first iteration) and The Lincoln Electric Co. (second and third iterations) for their assistance in manufacturing the experimental SMAW electrodes and preparing the test specimens. The authors also acknowledge the collaboration of the Welding Branch at NSWC-CD.

References

1. Evans, G. M. 1980. Effect of manganese on the microstructure and properties of all-weld-metal deposits. *Welding Journal* 59(3): 67-s to 75-s.

2. Evans, G. M. 1992. The effect of silicon on the microstructure and properties of C-Mn all-weld deposit. *WRA*, Vol. XXXVII, no. 2/3, pp. 20–31.

3. Suzuki, M., Tsukada, K., and Watanabe, I. 1982. Newly developed arctic grade high Al/low N/micro Ti type offshore structure steel. *Proceedings from London Conference Offshore Welded Structure.*

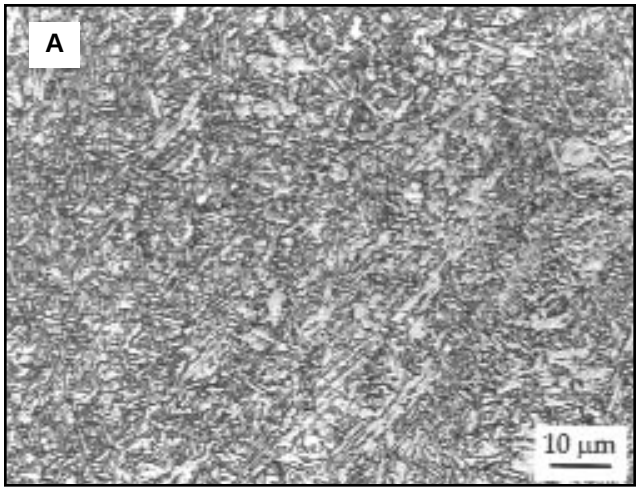

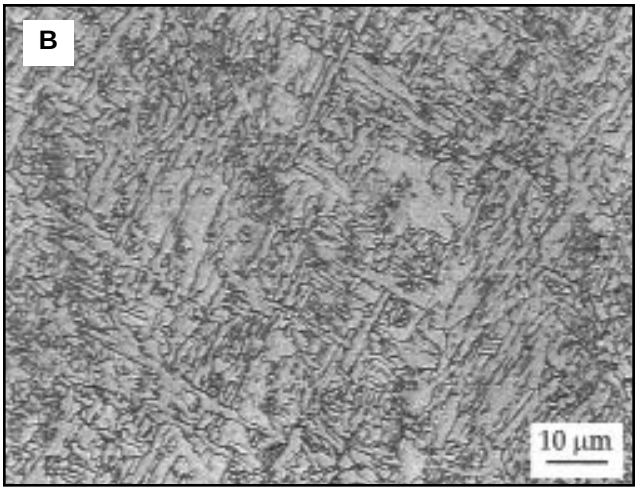

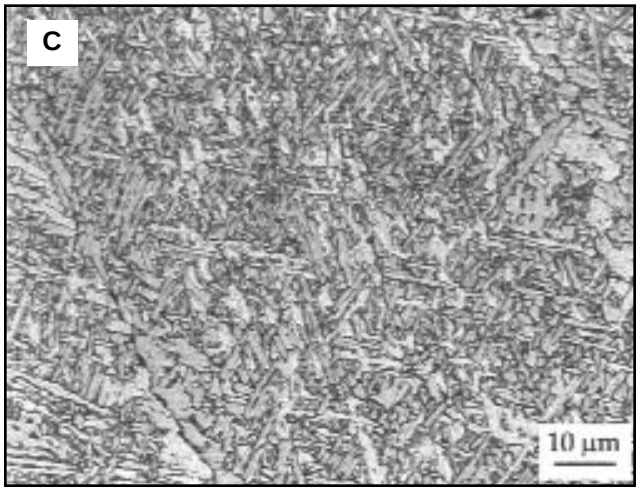

Fig. 19 — Micrographs of weld metals. A — A3-1; B — B3-1; C — C3-1.

4. Grong, O., and Matlock. 1985. Unpublished research. Colorado School of Mines, Golden, Colo.

5. Brownlee, J. K. 1985. Effects of aluminum and titanium on the microstructure and properties of microalloyed steel weld metal. Master's thesis. Colorado School of Mines, Golden, Colo.

6. Evans, G. M. 1992. The effects of aluminum on the microstructure and properties of C-Mn all welded metal deposits. *WRA* ,Vol. XXXVII, no. 8/9, pp. 2–12.

7. Snyder, J. P., II, and Pense, A. W., 1985. The effect of titanium on submerged arc weld metal. *Welding Journal* 61(7): 201-s to 211-s.

8. Johnson, M. Q. 1996. Microstructure-property relationships in titanium-bearing high-strength multipass shielded metal arc welding. Ph.D. thesis. Colorado School of Mines, Golden, Colo.

9. Evans, G. M. 1992. The effect of titanium on the microstructure and properties of C-Mn all-weld-metal deposits. *WRA*, Vol. XXXVIII, no. 8/9, pp. 13–21.

10. Liu, S., and Liao, F. C. 1997. Precipitates stability in the heat-affected zone of nitrogen enhanced high strength low alloy steels. *Materials Science & Engineering A*, 244(1998), pp. 273–283.

11. Mori, N., Homma, H., Okita, S., and Asano, K. The behavior of B and N in notch toughness improvement of Ti-B bearing weld metals. IIW/IIS-IX-1158-80.

12. Evans, G. M. 1996. Microstructure and properties of ferritic steel welds containing Ti and B. *Welding Journal* 75(8): 251-s to 260-s.

13. Oh, D. W., Olson, D. L., and Frost, R. H. 1990. The influence of boron and titanium on low-carbon steel weld metal. *Welding Journal* 69(4): 151-s to 158-s.

14. Evans, G. M. 1998. Effect of nitrogen on C-Mn steel welds containing titanium and boron. *Welding Journal* 77(5): 239-s to 248-s.

15. Sanchez-Osio, A., Liu, S., Ibarra, S., and Olson, D. L. 1995. Designing shielded metal arc consumables for underwater wet welding in offshore applications. *ASME Journal of Offshore Mechanics and Arctic Engineering* 117(8): 212–220.

16. Evans, G. M. 1991. The effect of chromium on microstructure and properties of C-Mn all weld metal deposits. *WRA*, Vol. XXXVII, no. 2/3, pp. 65–69.

17. Evans, G.M. 1991. The effect of molybdenum on microstructure and properties of C-Mn all weld metal deposits. *WRA*, Vol. XXXVII, no. 2/3, pp. 42–54.

18. Evans, G. M. 1991. The effect of nickel on microstructure and properties of C-Mn all weld metal deposits. *WRA*, Vol. XXXVII, no. 2/3, pp. 70–83.

19. Zhang, Z., and Farrar, R. A. 1997. Influence of Mn and Ni on the microstructure and toughness of C-Mn-Ni weld metals. *Welding Journal* 76(5): 183-s to 190-s.

20. Es-Souni, M., Beaven, P. A., and Evans, G. M. 1991. Microstructure and mechanical properties of Cu-bearing MMA C-Mn weld metal. *WRA*, Vol. XXXVII, no. 2/3, pp. 84–95.

21. Thompson, S. W., and Krauss, G. 1996. Austenite decomposition during continuous cooling of an HSLA-80 plate steel. *Metallurgical and Materials Transactions A*, Vol. 27A, June, pp. 1557–1571.

22. Kirshnadev, M. R., Zhang, W. L., Rene, Gendron, A., Vaidy, V., and Bowker, J. T. 1995. Influence of composition and cleanliness of electrodes on the weld metal properties and microstructure in advanced copper precipitation strengthened HSLA steels. *Proceedings of the International Symposium on High Performance Steels for Structural Applications*, Cleveland, Ohio, pp. 189–196.

23. Hannerz, N. E. 1987. Review on the influence of copper content on weld metal properties. IIW doc. IX-1487-87.

24. Habraken, L. J., and Economopous, M. 1967. Transformation hardenability in steels. Ann Arbor, Mich.: Climax Molybdenum Co., p. 81.

25. Thompson, S. W. 1993. Austenite transformation behavior and fracture performance of low-carbon, copper-containing steels with bainitic microstructures. Research report in CSM.

26. Ramirez, E., Liu, S., and Olson, D. L. 1996. Dual precipitation strengthening effect of copper and niobium in high-strength steel weld metal. *Materials Science and Engineering A*, A216, pp. 91–103, Oct.

27. Flemming, D. A., Barcarence, A. Q., Liu, S., and Olson, D. L. 1996. Toward developing a SMA welding electrode for HSLA-100 grade steel. *Welding Journal* 75(6): 171-s to 183-s.

28. Private communication with NSWC in 1994.